


Cite this: *Analyst*, 2021, **146**, 1859

## A stepwise recognition strategy for the detection of telomerase activity *via* direct electrochemical analysis of metal–organic frameworks

Jiarui Yang,<sup>a</sup> Pengfei Dong,<sup>a</sup> Yikun Wang,<sup>\*b</sup> Tianrui Liu,<sup>a</sup> Yuanyuan Huang<sup>a</sup> and Jianping Lei <sup>\*a</sup>

The detection of telomerase is of great significance for monitoring cell canceration. The conventional methods depend on the extension of telomerase towards its primer to conduct signal transduction. Herein, a specific and reliable detection strategy based on stepwise recognition was developed for tandem detection of metal ions and enzymes. We first synthesized an electrically active metal–organic framework (MIL-101(Fe)), which can act directly as a signal reporter in phosphate buffered saline after being modified with capture DNA (cDNA). When the zinc ion is added as a coenzyme factor, the modified hairpin DNA on the electrode is cleaved by DNAzyme to yield the activated primer. After the addition of telomerase, the cleaved DNA strand would be extended, and the resulting sequence will be hybridized with the signal label of MIL-101(Fe)–cDNA. Therefore, a signal-on strategy for the detection of telomerase was achieved based on the direct electrochemical analysis of MIL-101(Fe). Moreover, this electrochemical biosensor can discriminate telomerase activity among different cell lines. The stepwise recognition ensured the advantages of an electrochemical biosensor such as high sensitivity and specificity during the detection process, providing a novel method for monitoring and diagnosis of diseases.

Received 17th November 2020,  
Accepted 14th December 2020

DOI: 10.1039/d0an02233k

[rsc.li/analyst](http://rsc.li/analyst)

## Introduction

Metal–organic frameworks (MOFs) as an emerging material have attracted extensive attention in separation,<sup>1,2</sup> energy storage,<sup>3</sup> biopharmaceutical delivery,<sup>4,5</sup> catalysis,<sup>6–8</sup> and biosensors.<sup>9,10</sup> In particular, due to their large surface area and high mass transfer capacities, MOFs have shown promising potential in electrochemical biosensing. However, their poor conductivity and less selectivity blocked their further application in electrochemical biosensing. By introducing a highly active redox center into MOF materials, electrochemical sensors can realize ultra-sensitive detection of different analytes. For instance, by covalently modifying ferrocene to NH<sub>2</sub>-UiO-66 (University of Oslo), the constructed electrochemical sensing platform can achieve simultaneous and sensitive detection of Cu<sup>2+</sup>, Cd<sup>2+</sup> and Pb<sup>2+</sup>.<sup>11</sup> Secondly, MOFs and their composite materials with catalytic properties could act as a sensing platform for electrochemical biosensors as well.<sup>12,13</sup>

For example, by introducing PtNi alloy nanoclusters into MIL (Materials of Institute Lavoisier)-101 units, an electrochemical sensor was constructed to catalyze the reduction of methylene blue, thereby detecting NF-κB p50.<sup>14</sup> A porphyrin MOF with excellent catalytic capacity was utilized as a high-activity catalyst to electrocatalyze the reduction of O<sub>2</sub>, which was applied to the electrochemical evaluation of telomerase activity.<sup>15</sup> Compared with horseradish peroxidase, using the Cu-hemin MOF/chitosan-reduced graphene oxide nanocomposite with peroxidase-like activity as the signal tag could result in good catalytic activity for the reduction of H<sub>2</sub>O<sub>2</sub>.<sup>16</sup> The above methods used decorated MOFs as a signal label to complete the bioassay. Most recently, an electroactive MOF as a crystallized electrochemiluminescence (ECL) emitter was designed by using mixed ligands of hydroquinone and phenanthroline as oxidative and reductive couples, respectively.<sup>17</sup> Therefore, the primitive MOF could be utilized as the signal reporter to directly and conveniently construct a platform in biosensing.

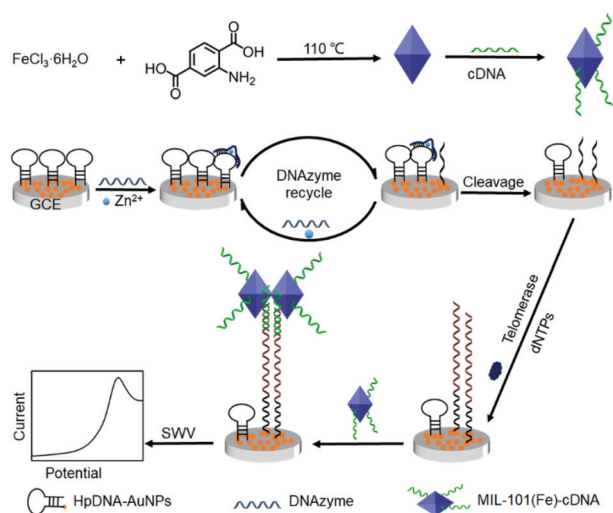
Telomerase is a basic nucleoprotein reverse transcriptase responsible for extending telomeres.<sup>18,19</sup> In normal cells, telomerase is inactive after cell division; in contrast, telomerase is abnormally expressed in cancer cells. Therefore, it is considered as a biomarker for the diagnosis of cell canceration.<sup>20,21</sup> Over the years, a wide range of methods have

<sup>a</sup>State Key Laboratory of Analytical Chemistry for Life Science, School of Chemistry and Chemical Engineering, Nanjing University, Nanjing 210023, China. E-mail: [jpl@nju.edu.cn](mailto:jpl@nju.edu.cn)

<sup>b</sup>Jiangsu Institute of Metrology, Nanjing 210023, China. E-mail: [wyk\\_jsmi@hotmail.com](mailto:wyk_jsmi@hotmail.com)

been developed to monitor telomerase activity, including the classic polymerase chain reaction technique,<sup>22</sup> and fluorescence,<sup>23–27</sup> ECL,<sup>28–31</sup> and electrochemical detection.<sup>32–36</sup> For example, a telomerase extension-triggered DNA walker was constructed, after DNA configuration transformation, and a molecular beacon tagged with Cy5 was released.<sup>37</sup> By combining telomerase extension and DNA cycle amplification techniques, ECL biosensors realized the ultrasensitive detection of telomerase.<sup>38</sup> Based on the electrocatalytic oxidation of CeMOFs towards hydroquinone to *p*-benzoquinone, a ratio-metric electrochemical biosensor was developed for monitoring telomerase.<sup>39</sup> These strategies based on telomerase extension to trigger the signal transduction provide an effective and sensitive method for detecting telomerase activity.

To further improve the specificity of biosensors, a stepwise recognition strategy was designed for the detection of telomerase activity *via* direct electrochemical analysis of primitive MOFs (Scheme 1). First, a MOF was synthesized by solvent thermal synthesis at 110 °C and then functionalized with capture DNA (cDNA) to obtain a signal label (MIL-101(Fe)-cDNA). Meanwhile, a sensing platform was constructed by modifying HpDNA-conjugated gold nanoparticles (AuNPs) on a glassy carbon electrode (GCE), which was cut by DNase in the presence of coenzyme zinc ions. The cleaved DNA terminal as the primer can be extended under the action of telomerase, and the extended sequence can be recognized by the MOF tags through the principle of base complementary pairing, leading to a stepwise recognition strategy for highly efficient electrochemical detection of telomerase activity. This strategy innovatively combines the merits of both MOFs and telomerase extension and realizes excellent discrimination in different cell lines, providing a new approach for designing highly specific and reliable biosensors.



**Scheme 1** Schematic diagram of the preparation of MIL-101(Fe)-cDNA tags and the stepwise recognition strategy for detection of telomerase.

## Experimental

### Materials and reagents

Aminoterephthalic acid (NH<sub>2</sub>-BDC), *N*-hydroxysuccinimide (NHS) and 1-(3-(dimethylamino)propyl)-3-ethylcarbodiimide hydrochloride (EDC) were obtained from Bide Pharmatech Ltd. Iron(III) chloride hexahydrate (FeCl<sub>3</sub>·6H<sub>2</sub>O) was obtained from Sigma-Aldrich (St Louis, MO, USA). Tetrachloroauric acid (HAuCl<sub>4</sub>) and trisodium citrate were purchased from Sinopharm Chemical Reagent Co., Ltd. A human telomerase (TE) ELISA kit was purchased from Qiaodu Biotechnology Co. Ltd. K562 cells were obtained from KeyGen Biotech Co., Ltd (Nanjing, China). The deoxynucleotide solution mixture (dNTPs) was obtained from KeyGen Biotech Co., Ltd. All DNA sequences were synthesized by Sangon Biological Engineering Technology Co., Ltd. The DNA sequences are as follows:

Hairpin DNA: 5'-GAGTGCATAATCCGTCGAGCAGAGTT/rA/GGAA-GATGGCATGCACTC-SH-3'.

DNase: 5'-GCCATCTTACGGAACCAGAGGACGAAAACCTCT-GC-3'.

cDNA: 5'-COOH-TTTTTTTTTTTTAAACCCTAACCTAACCT-3'.

### Synthesis of MIL-101(Fe)

The synthesis of MIL-101(Fe) is based on a previous report.<sup>40–42</sup> Briefly, 0.675 g of FeCl<sub>3</sub>·6H<sub>2</sub>O and 0.2246 g of NH<sub>2</sub>-BDC were dissolved in 15 mL of DMF in an autoclave, and then the mixture was heated at 110 °C for 24 h. After centrifugation and rinsing with DMF at 4000 rpm for 20 min, the obtained MIL-101(Fe) was dried in a vacuum at 110 °C.

### Bioconjugation of MIL-101(Fe)-cDNA

MIL-101(Fe)-cDNA was synthesized *via* an amide reaction between the -NH<sub>2</sub> group of MIL-101(Fe) and the -COOH group of cDNA.<sup>43</sup> 50 µL of cDNA (10 µM) was added to 450 µL of 400 mM EDC and 100 mM NHS in ultrapure water and shaken for 30 min at room temperature. Then 500 µL of MIL-101(Fe) aqueous solution (2 mg mL<sup>-1</sup>) was added into the above aqueous solution and reacted for 50 min at room temperature. The obtained mixture was washed at 4000 rpm for 20 min, and the unbound DNA was removed. The resulting MIL-101(Fe)-cDNA was resuspended in ultrapure water and stored at 4 °C.

### Synthesis of hairpin DNA-AuNPs (HpDNA-AuNPs)

27 nm-AuNPs were first synthesized according to the sodium citrate reduction method.<sup>44,45</sup> 1.15 mL of trisodium citrate aqueous solution (1%, w/v) was added to 50 mL of boiling HAuCl<sub>4</sub> solution (0.02%, w/v) rapidly under vigorous stirring. The above mixture was kept for boiling and stirred for 30 min and then naturally cooled to room temperature. The obtained AuNPs were filtered with a 0.22 µm sterile syringe filter and stored at 4 °C.

The HpDNA-AuNPs were assembled *via* Au-S bonding. 150 µL of HpDNA was added to 350 µL of AuNPs solution, and then the mixture was kept in a freezer (-20 °C) for 2 h.

## Gel electrophoresis analysis

2  $\mu\text{L}$  of  $6\times$  loading buffer was added to 7.0  $\mu\text{L}$  of DNA sample to prepare the loading sample, and then 9  $\mu\text{L}$  of the mixture was injected into 15% polyacrylamide gel. Gel electrophoresis was run at 110 V for 70 min in  $1\times$  TBE buffer. After dyeing with GelRed for 30 min, the gel was observed with Molecular Imager Gel Doc XR (BIO-RAD, USA).

## Electrochemical measurements

Initially, GCE (3 mm in diameter) was polished with 0.05  $\mu\text{m}$  alumina suspension, followed by sonication with pure water and ethanol, and it was washed and dried at room temperature. Subsequently, 5  $\mu\text{L}$  of HpDNA-AuNPs (3.5  $\mu\text{M}$ ) was dropped onto the clean electrode for 2 h at 37  $^{\circ}\text{C}$ . Then, 10  $\mu\text{L}$  of a mixture of DNAzyme and  $\text{Zn}^{2+}$  was added on the modified GCE electrode at 37  $^{\circ}\text{C}$  for 80 min. Next, 10  $\mu\text{L}$  of a mixture of pure telomerase or telomerase extract and dNTPs in TRAP buffer (20 mM Tris-HCl pH = 8.3, 1.5 mM  $\text{MgCl}_2$ , 63 mM KCl, 0.005% Tween 20, 1 mM EGTA, BSA 0.1  $\text{mg mL}^{-1}$ ) was added on the pre-treated electrode. After incubation at 37  $^{\circ}\text{C}$  for 80 min, the electrode was washed gently using 100  $\mu\text{L}$  of Tris-HCl (pH = 7.5) solution and reacted with 10  $\mu\text{L}$  of MIL-101(Fe)-cDNA at 37  $^{\circ}\text{C}$  for 90 min. Again, the electrode was washed gently using 100  $\mu\text{L}$  of Tris-HCl (pH = 7.5) solution.

The biosensor was evaluated with square wave voltammetry (SWV) in 0.1 M PBS solution from 0.2 V to 1.0 V with an amplitude of 25 mV and a frequency of 15 Hz. The resulting GCE electrode was used as the working electrode, the saturated calomel electrode was used as the reference electrode, and the platinum wire electrode was used as the counter electrode.

## Results and discussion

### Characterization of MIL-101(Fe)-cDNA and HpDNA-AuNPs

PXRD was employed to characterize the structure of MIL-101(Fe), Fig. 1A, and the characteristic peaks were observed at  $8.3^{\circ}$ ,  $8.8^{\circ}$ , and  $10.2^{\circ}$ , indicating a high crystallinity.<sup>46</sup> The morphology and structure of MIL-101(Fe) shown in TEM images indicated that the octahedron MOF is about 120 nm in size (Fig. 1B). To prepare the electrochemical tags, the cDNA was conjugated to the MOF *via* an amide reaction. As shown in Fig. 1C, the UV characteristic absorption peak of DNA is observed at 260 nm (curve b), while the MOF exhibits wide but weak absorption Q bands (curve a). After conjugating, the absorption of MIL-101(Fe)-cDNA with more negative charge demonstrated both the absorption at 260 nm and Q bands, corresponding to DNA and MOF respectively, proving that MIL-101(Fe)-cDNA tags were successfully synthesized for signal readout.

To demonstrate that HpDNA was loaded onto AuNPs, DLS and UV-vis spectra were utilized. In Fig. 1D, the average particle size distribution of AuNPs was 27 nm. Upon the modification of HpDNA, the DLS of HpDNA-AuNPs increased to 37 nm (Fig. 1E). Meanwhile, compared with the individual characteristic absorption peaks of HpDNA and AuNPs at 260

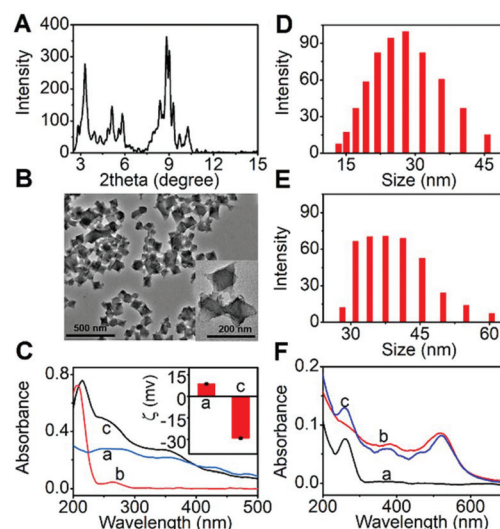


**Fig. 1** (A) PXRD pattern and (B) TEM image of MIL-101(Fe). (C) UV-vis spectra of MIL-101(Fe) (a), cDNA (b), and MIL-101(Fe)-cDNA (c). Inset: the zeta potential of (a) and (c). DLS analysis of (D) AuNPs and (E) HpDNA-AuNPs. (F) UV-vis spectra of AuNPs (a), HpDNA (b), and HpDNA-AuNPs (c).

and 520 nm, HpDNA-AuNPs have both characteristic peaks of HpDNA and AuNPs (Fig. 1F). The as-prepared HpDNA-AuNPs could be used as the substrate to modify the electrode for biorecognition.

### Feasibility of the biosensor

To verify the feasibility of the biosensor, square wave voltammetry was used for the detection of electrical activity of the MIL-101(Fe). Compared with the bare electrode (Fig. 2A-a), both the ligand-modified electrode (Fig. 2A-b) and MIL-101(Fe) modified electrode (Fig. 2A-c) showed large oxidation peaks at +0.82 V, which was attributed to the direct oxidation of the amino-group of  $\text{NH}_2\text{-BDC}$  ligands.<sup>47</sup> Moreover, compared with free ligands, the oxidation current of MIL-101(Fe) improved to 1.4 fold due to the framework structure.<sup>17</sup> It could be concluded that the MOF can act directly as a signal reporter. To evaluate the feasibility of stepwise recognition, linear sweep voltammetry (LSV) was performed in PBS. As shown in Fig. 2B,

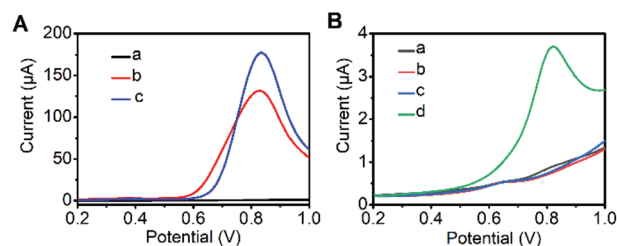


**Fig. 2** (A) SWV responses of the bare GCE (a),  $\text{NH}_2\text{-BDC}/\text{GCE}$  (b), and MIL-101(Fe)/GCE (c). (B) LSV responses of the electrochemical biosensor with the MIL-101(Fe)-cDNA tag in the absence (a) and presence of  $\text{Zn}^{2+}$  (b), telomerase (c), and telomerase and  $\text{Zn}^{2+}$  (d) in 0.1 M PBS.

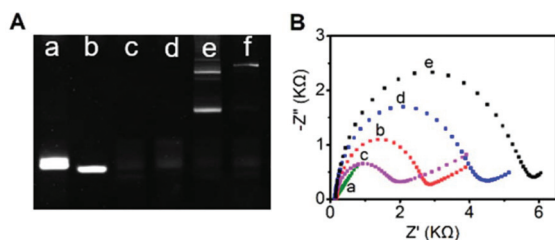


**Fig. 3** (A) PAGE analysis of HpDNA (lane a), cDNA (lane b), HpDNA + Zn<sup>2+</sup> + DNAzyme (lane c), HpDNA + DNAzyme (lane d), HpDNA + Zn<sup>2+</sup> + DNAzyme + telomerase + dNTPs (lane e), and HpDNA + Zn<sup>2+</sup> + DNAzyme + telomerase + dNTPs + cDNA (lane f). (B) EIS of the bare GCE (a), HpDNA–AuNPs modified GCE (b), followed by cleavage by DNAzyme (c), and then incubation with telomerase (d), and hybridization with MIL-101(Fe)–cDNA (e) in the solution containing 5.0 mM [Fe(CN)<sub>6</sub>]<sup>3−/4−</sup> and 0.1 M KCl.

in the case where neither the zinc ion nor telomerase is added, LSV demonstrated no obvious peak current. When the zinc ion and telomerase were added simultaneously, a large current peak appeared at 0.82 V, suggesting that the stepwise recognition is necessary for the signal enhancement.

In order to further verify the feasibility of the biosensor, polyacrylamide gel electrophoresis (PAGE) was carried out at 110 V for 70 min (Fig. 3A). The length of the DNA strand was negatively correlated with the immigration rate of the band. Lane a and lane b represent HpDNA and cDNA, respectively. Compared with lane d, there was a faster strand in lane c, which suggested that there was a new short strand of DNA. The above data indicated that HpDNA was only cleaved when Zn<sup>2+</sup> and DNAzyme were added together. Slower new bands appeared in lane e and lane f, which can be attributed to that the DNA strand was extended and then hybridized with cDNA, after adding telomerase, dNTPs, and cDNA. These results confirmed that the extension depends on the activation of the prime cleaved by the Zn<sup>2+</sup>–DNAzyme.

Electrochemical impedance spectra (EIS) were employed to measure the impedance of the modified electrode (Fig. 3B), and the diameter of the semicircle signal is positively correlated with the impedance of the electrode surface. When HpDNA–AuNPs (curve b) was modified on the GCE, the impedance on the electrode surface increased significantly relative to the bare electrode (curve a). After HpDNA was cleaved by Zn<sup>2+</sup> and DNAzyme, the signal value of the impedance decreased (curve c), which was attributed to the shorter length of the DNA strand on the electrode surface. Telomerase extended the length of DNA, which caused the increase of EIS signal (curve d). The extended DNA conjugated to MIL-101(Fe)–cDNA tags and further increased the impedance of the electrode (curve e).

### Optimization of conditions

In order to achieve the optimal detection performance of the biosensor, several important experimental conditions were optimized. The concentration of HpDNA on the electrode is one of the essential parameters affecting the current value.

The current was incremented with the increasing concentration, and it reached its maximum value at a concentration of 3.5 μM and then decremented. This was due to the fact that the excess DNA blocks the charge transfer on the electrode surface (Fig. 4A). Cleavage time is an important parameter that affects the experimental results. With the increase of cleavage time, the current curve first gradually increased and then flattened out after 80 min (Fig. 4B). With the increase of extending time, the signals increased and then decreased when the time is more than 80 min, which may be attributed to that longer strands of DNA block the charge transfer on the electrode surface (Fig. 4C). The signal intensity enhanced as the hybridization time increased and then became stable after 45 min (Fig. 4D). Therefore, the optimal experimental conditions were set to the concentration of 3.5 μM, the cleavage time of 80 min, the extension time of 80 min, and the hybridization time of 45 min.

### Electrochemical detection of Zn<sup>2+</sup> and telomerase activity

Under the optimal experimental conditions, SWV was carried out to detect Zn<sup>2+</sup> and telomerase activity. The peak value of current was related to the concentration of Zn<sup>2+</sup>; as the concentration of Zn<sup>2+</sup> increased, the current value increased (Fig. 5A). As shown in Fig. 5B, the peak currents had a good linear correlation with the logarithm of the concentration of Zn<sup>2+</sup> solution across the range from 1 × 10<sup>−10</sup> M to 1 × 10<sup>−5</sup> M. The regression equation is  $I$  (μA) = 0.72 Log( $C$ ) + 7.71, and the limit of detection was 2.2 × 10<sup>−11</sup> M. The biosensor exhibited excellent specificity in the detection of metal ions, which was attributed to that HpDNA can be cleaved by DNAzyme only when Zn<sup>2+</sup> was present (Fig. 5C).

As shown in Fig. 6A, the peak current changed with the added telomerase concentration. The peak currents had a good linear correlation with the logarithm of the concentration of the human telomerase standard across the range from 1 × 10<sup>−6</sup> IU L<sup>−1</sup> to 5 × 10<sup>−2</sup> IU L<sup>−1</sup>, which was wider than that using the ratiometric electrochemical method.<sup>39</sup> The

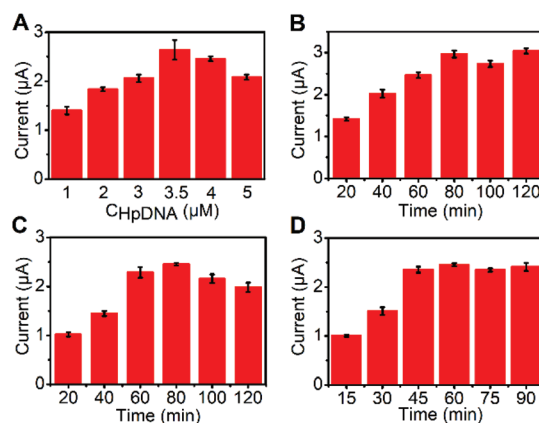


**Fig. 4** Effects of (A) concentration of HpDNA, (B) time for cleavage, (C) incubation time for telomerase extension reaction, and (D) hybridization time on currents in the electrochemical biosensing system.



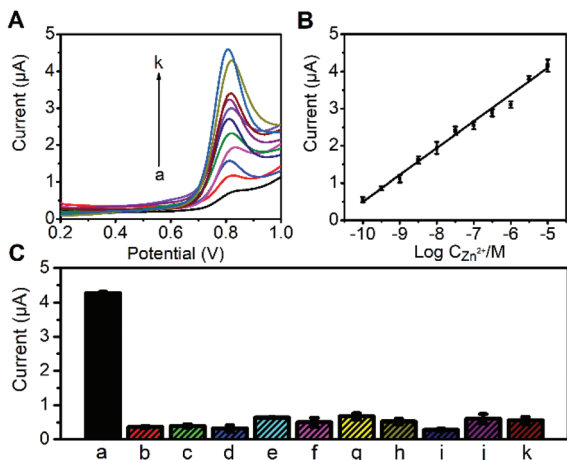


**Fig. 5** (A) SWV responses of the electrochemical biosensor at 0.1, 0.5, 1.0, 5.0, 10, 50,  $1 \times 10^2$ ,  $5 \times 10^2$ ,  $1 \times 10^3$ ,  $5 \times 10^3$ , and  $1 \times 10^4$  nM Zn<sup>2+</sup>. (B) Linear relationship between current and the concentration of Zn<sup>2+</sup>. (C) The detection towards other metal ions, 5 μM Zn<sup>2+</sup> (a), blank (b), Fe<sup>3+</sup> (c), Co<sup>3+</sup> (d), Ni<sup>2+</sup> (e), Cu<sup>2+</sup> (f), Cd<sup>2+</sup> (g), K<sup>+</sup> (h), Al<sup>3+</sup> (i), Mg<sup>2+</sup> (j), and Mn<sup>2+</sup> (k).

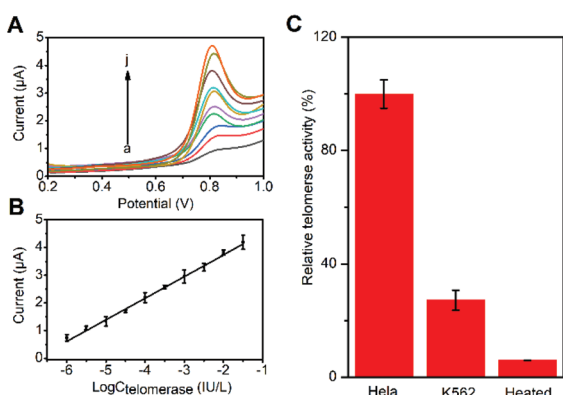


**Fig. 6** (A) SWV responses of the electrochemical biosensor at  $1 \times 10^{-6}$ ,  $5 \times 10^{-6}$ ,  $1 \times 10^{-5}$ ,  $5 \times 10^{-5}$ ,  $1 \times 10^{-4}$ ,  $5 \times 10^{-4}$ ,  $1 \times 10^{-3}$ ,  $5 \times 10^{-3}$ ,  $1 \times 10^{-2}$  and  $5 \times 10^{-2}$  IU L<sup>-1</sup> human telomerase standard solution. (B) Linear relationship between current and the concentration of telomerase. (C) The detection of extracts from HeLa, K562, and heated HeLa cells.

regression equation is  $I (\mu A) = 0.78 \log(C) + 5.29$ , and the limit of detection was  $1.8 \times 10^{-7}$  IU L<sup>-1</sup>. In order to verify the practical application effect of the biosensor, HeLa cell extract, K562 cell extract and heated HeLa cell extracts were examined. The results showed that HeLa cells show the highest telomerase activity.<sup>15,27</sup> The average telomerase activity in each HeLa cell was  $1.16 \times 10^{-9}$  IU. Compared with the HeLa cells with high telomerase activity, the telomerase activity in K562 cells was at a low level. After being heated, the HeLa cells showed no telomerase activity. These results showed that the stepwise recognition strategy is a promising distinguishing method in the monitoring of telomerase activity in biological samples.

## Conclusions

In summary, we successfully developed a stepwise recognition strategy for the electrochemical evaluation of Zn<sup>2+</sup> and telomerase activity. The synthesized MOF could be used as a signal reporter with a large current in the detection process directly, which provides great convenience for the construction of biosensors. Both DNAzyme-triggered recycling and the MIL-101(Fe)-based electrochemical signal significantly amplified for signal readout, leading to high sensitivity. Moreover, the unique detection strategy *via* enzyme cleavage and telomerase extension ensures the high specificity of the electrochemical biosensor. The developed stepwise recognition strategy not only realized the sequential detection of metal ions and enzymes, but also provided a new methodology for biochemical detection.

## Author contributions

J.R. Yang, Y.K. Wang and J.P. Lei planned the projects, designed the experiments and wrote the manuscript. J.R. Yang performed the experiments, and P.F. Dong, T.R. Liu and Y.Y. Huang gave assistance. Y.K. Wang and J.P. Lei supervised and coordinated all investigators for this project. All authors discussed the results and commented on the manuscript.

## Conflicts of interest

There are no conflicts to declare.

## Acknowledgements

We gratefully acknowledge the National Key Research and Development Program of China (2018YFF0212802) and the National Natural Science Foundation of China (21675084).

## Notes and references

- Y. H. Wang, H. Jin, Q. Ma, H. Z. Mao, A. Feldhoff, X. Z. Cao, Y. S. Li, F. S. Pan and Z. Y. Jiang, *Angew. Chem., Int. Ed.*, 2020, **59**, 4365–4369.
- Q. Hou, S. Zhou, Y. Y. Wei, J. R. Caro and H. H. Wang, *J. Am. Chem. Soc.*, 2020, **142**, 9582–9586.
- Y. Li, Y. X. Xu, W. P. Yang, W. X. Shen, H. G. Xue and H. Pang, *Small*, 2018, **14**, 1704435.
- J. T. Liu, T. R. Liu, P. Du, L. Zhang and J. P. Lei, *Angew. Chem., Int. Ed.*, 2019, **58**, 7808–7812.
- J. T. Liu, J. Huang, L. Zhang and J. P. Lei, *Chem. Soc. Rev.*, 2021, DOI: 10.1039/D0CS00178C.
- L. Jiao, W. J. Yang, G. Wan, R. Zhang, X. S. Zheng, H. Zhou, S. H. Yu and H. L. Jiang, *Angew. Chem., Int. Ed.*, 2020, **59**, 20589–20595.

- 7 L. Jiao, R. Zhang, G. Wan, W. J. Yang, X. Wan, H. Zhou, J. L. Shui, S. H. Yu and H. L. Jiang, *Nat. Commun.*, 2020, **11**, 2831.
- 8 Y. N. Gong, L. Jiao, Y. Y. Qian, C. Y. Pan, L. R. Zheng, X. C. Cai, B. Liu, S. H. Yu and H. L. Jiang, *Angew. Chem., Int. Ed.*, 2020, **59**, 2705–2709.
- 9 T. Z. Liu, R. Hu, X. Zhang, K. L. Zhang, Y. Liu, X. B. Zhang, R. Y. Bai, D. L. Li and Y. H. Yang, *Anal. Chem.*, 2016, **88**, 12516–12523.
- 10 J. F. Chang, X. Wang, J. Wang, H. Y. Li and F. Li, *Anal. Chem.*, 2019, **91**, 3604–3610.
- 11 X. X. Wang, Y. X. Qi, Y. Shen, Y. Yuan, L. D. Zhang, C. Y. Zhang and Y. H. Sun, *Sens. Actuators, B*, 2020, **310**, 127756.
- 12 Z. Ye, Q. W. Wang, J. T. Qiao, K. Y. Xu and G. P. Li, *Analyst*, 2019, **144**, 2120–2129.
- 13 S. Shahrokhian and S. Ranjbar, *Analyst*, 2018, **143**, 3191–3201.
- 14 H. Yu, W. Zhang, S. C. Lv, J. Han, G. Xie and S. P. Chen, *Chem. Commun.*, 2018, **54**, 11901–11904.
- 15 P. H. Ling, J. P. Lei and H. X. Ju, *Anal. Chem.*, 2016, **88**, 10680–10686.
- 16 L. Wang, H. Yang, J. He, Y. Y. Zhang, J. Yu and Y. H. Song, *Electrochim. Acta*, 2016, **213**, 691–637.
- 17 Z. C. Jin, X. R. Zhu, N. N. Wang, Y. F. Li, H. X. Ju and J. P. Lei, *Angew. Chem., Int. Ed.*, 2020, **59**, 10446–10450.
- 18 L. Zou, X. H. Li, J. Zhang and L. S. Ling, *Anal. Chem.*, 2020, **92**, 12656–12662.
- 19 P. D. Garcia, R. W. Leach, G. M. Wadsworth, K. Choudhary, H. Li, S. Aviran, H. D. Kim and V. A. Zakian, *Nat. Commun.*, 2020, **11**, 2173.
- 20 Y. Ma, Z. H. Wang, Y. X. Ma, Z. H. Han, M. Zhang, H. Y. Chen and Y. Q. Gu, *Angew. Chem., Int. Ed.*, 2018, **57**, 5389–5393.
- 21 Y. Ma, Z. H. Wang, M. Zhang, Z. H. Han, D. Chen, Q. Y. Zhu, W. D. Gao, Z. Y. Qian and Y. Q. Gu, *Angew. Chem., Int. Ed.*, 2016, **55**, 3304–3308.
- 22 L. L. Tian and Y. Weizmann, *J. Am. Chem. Soc.*, 2013, **135**, 1661–1664.
- 23 Y. Zhuang, F. J. Huang, Q. Xu, M. S. Zhang, X. D. Lou and F. Xia, *Anal. Chem.*, 2016, **88**, 3289–3294.
- 24 X. X. Wang, D. D. Yang, M. Liu, D. W. Cao, N. Y. He and Z. F. Wang, *Biosens. Bioelectron.*, 2019, **137**, 110–116.
- 25 Z. M. Huang, M. Y. Lin, C. H. Zhang, Z. K. Wu, R. Q. Yu and J. H. Jiang, *Anal. Chem.*, 2019, **91**, 9361–9365.
- 26 X. W. Ou, S. S. Zhan, S. L. Sun, Y. Cheng, B. F. Liu, T. Y. Zhai, X. D. Lou and F. Xia, *Biosens. Bioelectron.*, 2019, **124–125**, 199–204.
- 27 R. C. Qian, L. Ding, L. W. Yan, M. F. Lin and H. X. Ju, *Anal. Chem.*, 2014, **86**, 8642–8648.
- 28 H. R. Zhang, B. X. Li, Z. M. Sun, H. Zhou and S. S. Zhang, *Chem. Sci.*, 2017, **8**, 8025–8029.
- 29 X. M. Zhou, D. Xing, D. B. Zhu and L. Jia, *Anal. Chem.*, 2009, **81**, 255–261.
- 30 H. R. Zhang, M. S. Wu, J. J. Xu and H. Y. Chen, *Anal. Chem.*, 2014, **86**, 3834–3840.
- 31 Q. M. Feng, Z. Zhou, M. X. Li, W. Zhao, J. J. Xu and H. Y. Chen, *Biosens. Bioelectron.*, 2017, **90**, 521–527.
- 32 Z. Yi, H. B. Wang, K. Chen, Q. Gao, H. Tang, R. Q. Yu and X. Chu, *Biosens. Bioelectron.*, 2014, **53**, 310–315.
- 33 L. Wang, T. J. Meng, G. S. Yu, S. S. Wu, J. J. Sun, H. X. Jia, H. Wang, X. J. Yang and Y. F. Zhang, *Biosens. Bioelectron.*, 2019, **124–125**, 53–58.
- 34 L. Wang, T. J. Meng, L. N. Liang, J. J. Sun, S. S. Wu, H. Wang, X. J. Yang and Y. F. Zhang, *Sens. Actuators, B*, 2019, **278**, 133–139.
- 35 L. Wang, T. J. Meng, D. Zhao, H. X. Jia, S. Y. An, X. J. Yang, H. Wang and Y. F. Zhang, *Biosens. Bioelectron.*, 2020, **148**, 111834.
- 36 X. Liu, M. Wei, E. S. Xu, H. T. Yang, W. Wei, Y. J. Zhang and S. Q. Liu, *Biosens. Bioelectron.*, 2017, **91**, 347–353.
- 37 J. Huang, L. Y. Zhu, H. X. Ju and J. P. Lei, *Anal. Chem.*, 2019, **91**, 6981–6985.
- 38 C. Y. Xiong, W. B. Liang, Y. N. Zheng, Y. Zhuo, Y. Q. Chai and R. Yuan, *Anal. Chem.*, 2017, **89**, 3222–3227.
- 39 P. F. Dong, L. Y. Zhu, J. Huang, J. J. Ren and J. P. Lei, *Biosens. Bioelectron.*, 2019, **138**, 111313.
- 40 Z. Y. Dong, Y. Z. S. Sun, J. Chu, X. Z. Zhang and H. X. Deng, *J. Am. Chem. Soc.*, 2017, **139**, 14209–14216.
- 41 D. K. Wang, R. K. Huang, W. J. Liu, D. R. Sun and Z. H. Li, *ACS Catal.*, 2014, **4**, 4254–4260.
- 42 Z. W. Jiang, P. F. Gao, L. Yang, C. Z. Huang and Y. F. Li, *Anal. Chem.*, 2015, **87**, 12177–12182.
- 43 X. X. Wang, Y. X. Qi, Y. Shen, Y. Yuan, L. D. Zhang, C. Y. Zhang and Y. H. Sun, *Sens. Actuators, B*, 2020, **310**, 127756.
- 44 Z. Yi, X. Y. Li, F. J. Liu, P. Y. Jin, X. Chu and R. Q. Yu, *Biosens. Bioelectron.*, 2013, **43**, 308–314.
- 45 J. W. Liu and Y. Lu, *Nat. Protoc.*, 2006, **1**, 246–252.
- 46 B. Y. Shen, X. Chen, K. Shen, H. Xiong and F. Wei, *Nat. Commun.*, 2020, **11**, 2692.
- 47 J. Y. Liu, L. Cheng, B. F. Liu and S. J. Dong, *Langmuir*, 2000, **16**, 7471–7476.